



**HAL**  
open science

## Simulation of 3D granular media by multiscale random polyhedra

Julie Escoda, Dominique Jeulin, François Willot

► **To cite this version:**

Julie Escoda, Dominique Jeulin, François Willot. Simulation of 3D granular media by multiscale random polyhedra. International Congress of Stereology, 2011, Beijing, China. <hal-00879260>

**HAL Id: hal-00879260**

**<https://minesparis-psl.hal.science/hal-00879260v1>**

Submitted on 4 Nov 2013

**HAL** is a multi-disciplinary open access archive for the deposit and dissemination of scientific research documents, whether they are published or not. The documents may come from teaching and research institutions in France or abroad, or from public or private research centers.

L'archive ouverte pluridisciplinaire **HAL**, est destinée au dépôt et à la diffusion de documents scientifiques de niveau recherche, publiés ou non, émanant des établissements d'enseignement et de recherche français ou étrangers, des laboratoires publics ou privés.



HAL Authorization

# SIMULATION OF 3D GRANULAR MEDIA BY MULTISCALE RANDOM POLYHEDRA

*J. Escoda<sup>1,2</sup>, D. Jeulin<sup>1</sup>, and F. Willot<sup>1</sup>*

<sup>1</sup> Centre de Morphologie Mathématique, Mathématiques et Systèmes, Mines ParisTech, Fontainebleau, France

<sup>2</sup> Département Matériaux et Mécanique des Composants, Electricité de France, Moret-sur-Loing, France

## ABSTRACT

In order to simulate granular microstructures such as cementitious materials, a Boolean Poisson polyhedra model is implemented. 3D images are generated as vector images for derivation of faster algorithms. Different morphological measurements (specifically covariance of mosaic and Boolean models, and geometrical covariogram of primary grains), which theoretical expressions are known for such models, are used to validate the algorithm.

**KEYWORDS:** random sets, microstructure, mathematical morphology, Poisson polyhedra, concrete

## I. INTRODUCTION

As it is not possible to investigate experimentally all types of concrete of EDF facilities, due to the large variability of such materials, modeling its behavior and hence its microstructure is necessary. To this purpose, this paper investigates the implementation of Boolean Poisson polyhedra models (see [3]). Such models could more be used more generally for other granular media.

Our implementation of the algorithm, given in section III, generates vector images, which allows faster computations. This implementation is validated in section IV where various morphological measurements (covariance of mosaic and Boolean models, and geometrical covariogram of primary grains) are computed on simulations and compared to theoretical expressions which are known for such a model.

## II. POISSON POLYHEDRA MODEL

Boolean models consist of the implantation of random primary grains located on Poisson points (see [2, 4]). Hence, the number of points on the image follows the Poisson distribution:

$$P\{n = k\} = \frac{e^{-N_0} N_0^k}{k!},$$

(1)

where  $N_0$  is the expectation distribution. Here, Poisson points are distributed uniformly on the image.

For a Boolean Poisson polyhedra random model (a realistic model for cementitious

materials), primary grains are made of Poisson polyhedra defined as follow. Each Poisson polyhedron is obtained from a Poisson tessellation of the image: Poisson planes with density  $\lambda$  are implanted on the image, i.e the number of planes hitting a sphere enclosing a cube with side  $L$  follows the Poisson distribution (1) with expectation  $N = 2\pi\sqrt{3}\lambda L$ . Poisson polyhedra are defined as the complementary set of this tessellation. Accordingly, a Poisson polyhedron is generated by randomly selecting (by number) one polyhedron among the polyhedra defined by the Poisson tessellation. In order to obtain a set of independent random Poisson polyhedra, each polyhedron is generated by a new realization of the space tessellation.

According to the classical relation for Boolean models, the volume fraction  $p$  and the primary grains average volume  $K_0$  are linked by:

$$p = 1 - e^{-\theta K_0}, \quad (2)$$

$\theta$  being the intensity of the Poisson points process, and the average volume for Poisson polyhedra being given by (see [2]):

$$K_0 = 6/\pi^4 \lambda^3. \quad (3)$$

## III. MODEL IMPLEMENTATION

### Space tessellation

First, the space tessellation is generated by generating  $N_p$  Poisson planes  $(P_i)_{i \leq N_p}$ ,  $N_p$  following the Poisson distribution (1). Each plane  $P_i$  is defined by a normal vector  $\mathbf{u}_i$  and a distance  $r_i$ . In order to obtain uniformly distributed planes and isotropic tessellations,  $\mathbf{u}_i$  follows a uniform distribution over the unit sphere, while  $r_i$  is

uniformly distributed between 0 and  $L\sqrt{3}/2$  (implantation of planes in the circumscribed sphere of the 3D image with side  $L$ ).

### Polyhedra labeling

Generating one Poisson polyhedron requires a labeling of the polyhedra obtained by the space tessellation, in order to select one polyhedron by number, not by volume (obtained for example by selecting the polyhedron containing one given point): each polyhedron needs to be specifically identified. Our algorithm generates vector images, i.e. defined analytically, in order to obtain faster realizations. Moreover, only polyhedra which are not cut by the edge of the image are labeled, to generate intact polyhedra.

Each polyhedron is completely known by its position with respect to each plane  $P_i$  of Cartesian equation  $\alpha_i x + \beta_i y + \gamma_i z + \delta_i = 0$ . Accordingly, in our algorithm, a polyhedron is labeled with a list of signs  $(s_i)_{i \leq N_p}$  such as  $s_i = 1$  (resp.  $s_i = -1$ ) if  $\alpha_i x_1 + \beta_i x_2 + \gamma_i x_3 + \delta_i > 0$  (resp.  $\alpha_i x_1 + \beta_i x_2 + \gamma_i x_3 + \delta_i < 0$ ) for all  $\mathbf{x} = (x_1, x_2, x_3)$  included in the polyhedron.

The algorithm iterates over straight lines  $(d_{i,j})_{i \leq N_p, i < j \leq N_p}$  in the image, corresponding to the pairs of plans  $(P_i, P_j)_{i \leq N_p, i < j \leq N_p}$ , in order to iterate over the edges of all polyhedra. The intersection between a given line  $d_{i,j}$  and each plane  $(P_k)_{k \leq N_p}$  allows to obtain a list of segments included in  $d_{i,j}$ . Each of these segments corresponds to the edge of four polyhedra which are then labeled with a list of signs  $(s_i)_{i \leq N_p}$ , directly computed from the position of the segment with respect to the list of planes  $(P_i)_{i \leq N_p}$ . Through this process, two lists of polyhedra known by their labels  $(s_i)_{i \leq N_p}$  are updated. These two lists correspond to polyhedra entirely included in the image, and polyhedra cut by the edge of the image respectively. This second list is used to ensure that the first one only contains intact polyhedra.

A 2D equivalent problem is represented in Fig. 1. In such a case, the iteration is carried out over Poisson lines and each segment of the line is an edge of two polygons.

### Miles-Lantuéjoul correction method

The next step of the algorithm is to select by

number one polyhedron from the labeling. As only polyhedra not cut by the edge of the image are taken into account while selecting a polyhedra on the 3D image, it is more likely to select small polyhedra than larger ones.

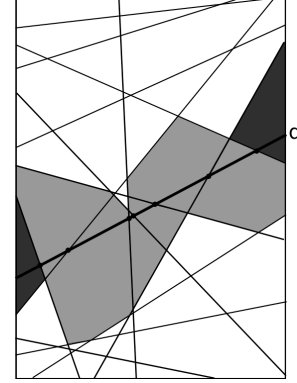


Figure 1: Polygons labeling in a 2D Poisson tessellation.

Iterations are carried out over Poisson lines. When considering the line  $d$ , light gray polygons are added to the list of intact polygons, if they are not member of the list of polygons cut by the edge of the image; while dark gray polygons are added to this second list and removed from the list of intact polygons.

Quantitatively, the probability for an object to have its bounding box  $B$  entirely included in a cube-shaped domain  $D$  is:

$$P[B \subset D] = \frac{(L - L_x)(L - L_y)(L - L_z)}{L^3},$$

(4)

where  $L$  is the side of the domain  $D$ , and  $L_x, L_y, L_z$  are the dimension of  $B$  (see Fig. 2).

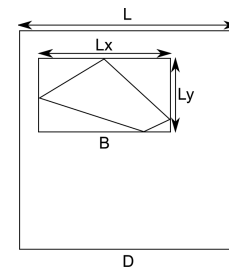


Figure 2: Miles-Lantuéjoul correction: probability for an object to have its bounding box  $B$  entirely included in a domain  $D$ .

To correct this bias, the selection of a polyhedron among a set of polyhedra involves weights  $1/P[B \subset D]$  instead of equiprobability (see [4]).

Binarization of a Boolean model realization

The Boolean model is obtained by the implantation of Poisson polyhedra on a Poisson points process on the 3D image. Polyhedra are binarized using their position with respect to each plane, i.e. their label  $(s_i)_{i \leq Np}$ . In order to efficiently binarize the image, each polyhedron is binarized on its bounding box and only planes defining boundaries of the polyhedra are considered among the list of planes  $(P_k)_{k \leq Np}$ . Indeed, necessary data for such a computation were saved during the polyhedra labeling. Last, the convexity of polyhedra is used to get a faster binarization. Instead of testing all points of the bounding box grid, each straight line of the grid of equation  $(x=x_i, y=y_j)_{i,j}$  is considered. Only points at the intersection of this line and the planes defining the polyhedron are tested: when two of these points are found to be on the boundaries of the polyhedron which is being binarized, all points of the grid between these two points are part of the polyhedron.

#### IV. IMPLEMENTATION VALIDATION

The aim of this section is to validate the implementation of the model given in section III using various morphological measurements which theoretical expressions are known for models using Poisson planes.

##### Geometrical covariogram

The geometrical covariogram is defined by:

$$K(h) = \bar{\mu}_3(A \cap A_{-h}), \quad (5)$$

and is equal, for Poisson polyhedra, to:

$$K(h) = K(0) \exp(-\pi \lambda h), \quad (6)$$

$K(0)=K_0$  being the average Poisson polyhedra volume (see Eq. 3), and  $\lambda$  being the Poisson planes intensity.

The geometrical covariogram is evaluated for different values of the expected number of planes  $N = 80, 100, 150, 300$  and for  $L=256$ . For each value, the geometrical covariogram is weighted by  $1/P[BCD]$  (see Eq. 4) as it is also done for polyhedra selection. When  $N=80, 100$  (resp.  $N=150, 200, 300$ ), the average geometrical covariogram is computed over 10000 (resp. 5000)

realizations. The relative error with respect to theoretical value, for corrected geometrical covariograms with  $h=0$  (i.e for average volume), is given in Tab. 1 and the geometrical covariogram for  $N=200$  is given in Fig. 3.

When  $N$  is low, the 3D space tessellation is not representative, and explains the observed error on the geometrical covariogram. Hence, a value of  $N=200$  is chosen for Boolean model realizations. To generate realizations of models with an intensity  $\lambda$  corresponding to an other value of  $N$ , a scaling is carried out.

Table 1: Relative error  $\varepsilon(K^{corr}(0))$  on corrected average Poisson polyhedra volume for different expected planes number  $N$ .

$N$	80	100	150	200	300
$\varepsilon(K^{corr}(0))$	73%	43%	14%	7%	6%

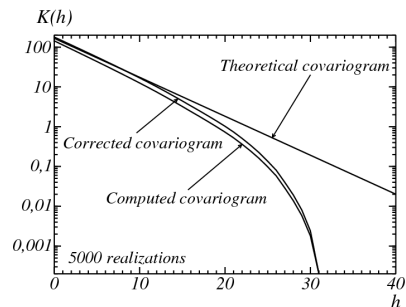


Figure 3: Geometrical covariogram for  $N=200$ . Theoretical covariogram as well as computed and corrected covariograms are given.

##### Poisson mosaic covariance

A binary Poisson mosaic model is realized, i.e. a Poisson tessellation is generated, and each polyhedra is set to value 1 (or 0) with a probability  $p$  (or  $1-p$  resp.). The theoretical covariance of such model (set A) is given by:

$$C(h) = P[\mathbf{x} \in A, \mathbf{x} + \mathbf{h} \in A] = pr(h) + p^2 r^2(h), \quad (7)$$

with  $r(h)=K(h)/K(0)$  the normalized geometrical covariogram of Poisson polyhedra.

Since the algorithm generates vector images, the covariance is evaluated without binarization, which introduces a bias, directly on the analytical data on random points of the 3D image.

For generated mosaic models with  $N=200$  and  $p=0.25$  (see a 2D cut of such a model in Fig. 4), the covariance is evaluated by taking 50000

points with a step  $L/256$  for  $h$ . This computation is carried out on twelve images (see Fig. 5, where theoretical and computed covariance are given).

### Boolean Poisson polyhedra covariance

Last, for Boolean models, the covariance of the complementary set is given by:

$$Q(h) = q^{2-r(h)},$$

(8)

with  $q=1-p$  (see Eq. 2 for the theoretical expression of  $p$ ).

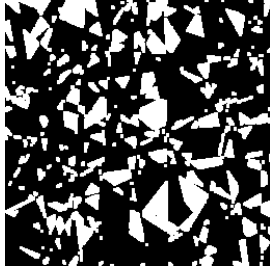


Figure 4: 2D cut of a binary Poisson mosaic of size  $256^3$  with  $p=0.25$  and  $N=200$ .

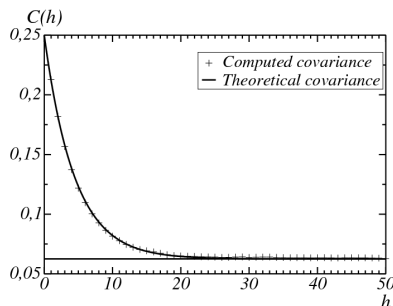


Figure 5: Theoretical and computed covariance of a Poisson polyhedra mosaic of parameters  $N = 200$  and  $p = 0.25$ . The asymptotic value  $p^2$  is given as a straight line.

A realization of a Boolean model is given in Fig. 6 where  $\lambda=0.045$  and  $p=0.2$ , for a 3D image of size  $500^3$ . The covariance is measured on the binarized image and is given in Fig. 7, with the theoretical covariance. For smaller values of  $\lambda$ , the 3D image obtained is not representative, and the computed covariance does not fit the theoretical covariance.

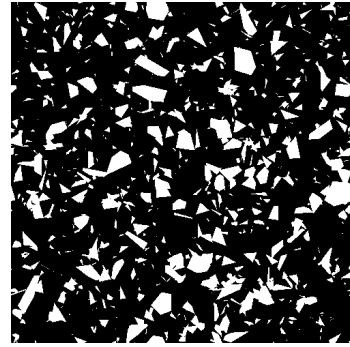


Figure 6: 2D cut of a Boolean Poisson polyhedra model of size  $500^3$  with  $\lambda=0.045$  and  $p=0.2$ .

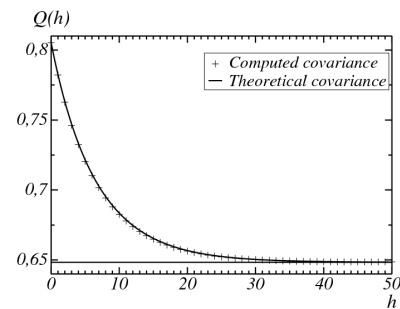


Figure 7: Theoretical and computed covariance of the complementary set of a Boolean Poisson polyhedra model of size  $500^3$  with  $\lambda=0.045$  and  $p=0.2$ . The asymptotic value  $p^2$  is given as a straight line.

## V. CONCLUSION

The vector implementation of Poisson polyhedra has been validated using various morphological measurements which are computed on simulated models and compared with theoretical expressions. It provides a bank of random polyhedra that can be implemented at any scale.

Such a model may be easily generalized to multiscale Boolean models to simulate cementitious material such as concrete. Their microstructure is known by morphological measurements carried out on segmented 3D real images obtained by microtomography (see [1]), and by experimental data such as granulometry. Then, the models parameters are numerically optimized using known analytical forms for the covariance, which allows for very fast computations of model samples, whereas the representative scales in the multiscale modeling are determined using the aggregates granulometry.

## REFERENCES

- [1] J. Escoda, F. Willot, D. Jeulin, J. Sanahuja, C. Toulemonde, "Estimation of local stresses and elastic properties of a mortar sample by FFT computation of fields on a 3D image", *Cement Concrete Res.*, Vol. 41(5), pp.542-556, 2011.
- [2] G. Matheron, "Random Sets and Integral Geometry", Wiley, 1975.
- [3] J.L. Quenec'h, M. Coster, J.L. Chermant, D. Jeulin, "Study of the liquid-phase sintering process by probabilistic models: application to the coarsening of WC-CO cermets", *J. Microsc.*, Vol. 168(1), pp.3-14, 1992.
- [4] J. Serra, "Image Analysis and Mathematical Morphology", Academic Press, 1982.